JCI The Journal of Clinical Investigation

An autoreactive antibody from an SLE/HIV-1 individual broadly neutralizes HIV-1

Mattia Bonsignori, … , John R. Mascola, Barton F. Haynes

J Clin Invest. 2014. https://doi.org/10.1172/JCI73441.

Research Article **Immunology**

Broadly HIV-1–neutralizing antibodies (BnAbs) display one or more unusual traits, including a longheavy chain complementarity-determining region 3 (HCDR3), polyreactivity, and high levels of somatic mutations. These shared characteristics suggest that BnAb development might be limited by immune tolerance controls. It has been postulated that HIV-1–infected individuals with autoimmune disease and defective immune tolerance mechanisms may produce BnAbs more readily than those without autoimmune diseases. In this study, we identified an HIV-1–infected individual with SLE who exhibited controlled viral load (<5,000 copies/ml) in the absence of controlling HLA phenotypes and developed plasma HIV-1 neutralization breadth. We collected memory B cells from this individual and isolated a BnAb, CH98, that targets the CD4 binding site (CD4bs) of HIV-1 envelope glycoprotein 120 (gp120). CH98 bound to human antigens including dsDNA, which is specifically associated with SLE. Anti-dsDNA reactivity was also present in the patient's plasma. CH98 had a mutation frequency of 25% and 15% nt somatic mutations in the heavy and light chain variable domains, respectively, a long HCDR3, and a deletion in the light chain CDR1. The occurrence of anti-dsDNA reactivity by a HIV-1 CD4bs BnAb in an individual with SLE raises the possibility that some BnAbs and SLE-associated autoantibodies arise from similar pools of B cells.

An autoreactive antibody from an SLE/HIV-1 individual broadly neutralizes HIV-1

Mattia Bonsignori,[1,2] Kevin Wiehe,[1,2] Sebastian K. Grimm,[3] Rebecca Lynch,[4] Guang Yang,[5] Daniel M. Kozink,[1,2] Florence Perrin,[1,2] Abby J. Cooper,[1,2] Kwan-Ki Hwang,[1,2] Xi Chen,[1,2] Mengfei Liu,[6] Krisha McKee,[4] Robert J. Parks,[1,2] Joshua Eudailey,[1] Minyue Wang,[1] Megan Clowse,[2] Lisa G. Criscione-Schreiber,[2] M. Anthony Moody,[1,7] Margaret E. Ackerman,[3] Scott D. Boyd,[8] Feng Gao,[1,2] Garnett Kelsoe,[1,5] Laurent Verkoczy,[1,2,9] Georgia D. Tomaras,[1,5,10] Hua-Xin Liao,[1,2] Thomas B. Kepler,[11] David C. Montefiori,[1,10] John R. Mascola,[4] and Barton F. Haynes[1,2,5]

[1]Duke Human Vaccine Institute and [2]Department of Medicine, Duke University Medical Center, Durham, North Carolina, USA. [3]Thayer School of Engineering, Dartmouth College, Hanover, New Hampshire, USA. [4]Vaccine Research Center, NIAID, NIH, Bethesda, Maryland, USA. [5]Department of Immunology, Duke University Medical Center, Durham, North Carolina, USA. [6]Duke University School of Medicine, Durham, North Carolina, USA. [7]Department of Pediatrics, Duke University Medical Center, Durham, North Carolina, USA. [8]Department of Pathology, Stanford University, Palo Alto, California, USA. [9]Department of Pathology and [10]Department of Surgery, Duke University Medical Center, Durham, North Carolina, USA. [11]Department of Microbiology, Boston University, Boston, Massachusetts, USA.

Broadly HIV-1–neutralizing antibodies (BnAbs) display one or more unusual traits, including a long heavy chain complementarity-determining region 3 (HCDR3), polyreactivity, and high levels of somatic mutations. These shared characteristics suggest that BnAb development might be limited by immune tolerance controls. It has been postulated that HIV-1–infected individuals with autoimmune disease and defective immune tolerance mechanisms may produce BnAbs more readily than those without autoimmune diseases. In this study, we identified an HIV-1–infected individual with SLE who exhibited controlled viral load (<5,000 copies/ml) in the absence of controlling HLA phenotypes and developed plasma HIV-1 neutralization breadth. We collected memory B cells from this individual and isolated a BnAb, CH98, that targets the CD4 binding site (CD4bs) of HIV-1 envelope glycoprotein 120 (gp120). CH98 bound to human antigens including dsDNA, which is specifically associated with SLE. Anti-dsDNA reactivity was also present in the patient's plasma. CH98 had a mutation frequency of 25% and 15% nt somatic mutations in the heavy and light chain variable domains, respectively, a long HCDR3, and a deletion in the light chain CDR1. The occurrence of anti-dsDNA reactivity by a HIV-1 CD4bs BnAb in an individual with SLE raises the possibility that some BnAbs and SLE-associated autoantibodies arise from similar pools of B cells.

Introduction

Broadly HIV-1–neutralizing antibodies (BnAbs) have been isolated that bind to multiple epitopes on the envelope glycoproteins gp120 and gp41 (reviewed in ref. 1). 2G12 recognizes a posttranslational glycan epitope on gp120 (2, 3). CH103–CH106 (4), b12 (5, 6), VRC01 (7), and numerous other mAbs with VRC01-like characteristics, such as VRC03, VRC-PG04, CH30–CH34, and the HAAD motif antibodies (7–9), recognize the CD4 binding site (CD4bs). HJ16 binds to an epitope near the CD4bs (10). PG9 and PG16, CH01–CH04, and PGT141–PGT145 recognize conformational epitopes in the gp120 V1/V2 region with binding dependence on V2 asparagine residue 160 (11–13). PGT121–PGT123, PGT135–PGT137, PGT125–PGT128, PGT130, and PGT131 recognize a diverse set of carbohydrate or carbohydrate-dependent epitopes in the gp120 V3 region (13). 3BC176 and 3BC315 recognize a conformational HIV-1 spike epitope in the proximity of the V3 loop and the CD4i site that is exposed in part by CD4 binding (14). Finally, 2F5 (2, 15, 16), 4E10 (2, 17), 10E8 (18), and Z13 (19) bind to the membrane proximal external region (MPER) of gp41.

Each of these antibodies displays one or more unusual characteristics, such as polyreactivity with human and/or nonhuman antigens, long heavy chain complementarity-determining region 3 (HCDR3) loops, and high levels of somatic mutations (1, 13, 20–23). These traits suggest that the development of these types of BnAbs may be limited by immune tolerance controls that impede the required tortuous or polyreactive BnAb maturation pathways (20, 21, 24). This notion is supported by a number of observations in 2F5 $V_H \times V_L$ knockin mice: targeted expression of the 2F5 V_HDJ_H/V_LJ_L rearrangements triggered a near-complete B cell developmental blockade at the pre-B to immature B cell stage (25); even when clonal deletion mechanisms were circumvented, 2F5 V_HDJ_H/V_LJ_L-expressing broadly neutralizing B cell rescue was limited by κ chain editing and an anergic phenotype (26); and MPER-specific serum neutralizing IgG responses were elicited in 2F5 knockin mice immunized with MPER-lipid complexes by rescuing the anergic self-reactive 2F5-expressing B cells that survived the B cell developmental blockade (26).

We have previously suggested that the paucity of subjects developing BnAbs may be due to the frequent deletion of B cell precursors that acquire autoreactivity during their maturation process (at either early or late stages) and hypothesized that HIV-1–infected subjects with autoimmune diseases might be capable of devel-

Conflict of interest: The authors have declared that no conflict of interest exists.

Note regarding evaluation of this manuscript: Manuscripts authored by scientists associated with Duke University, The University of North Carolina at Chapel Hill, Duke-NUS, and the Sanford-Burnham Medical Research Institute are handled not by members of the editorial board but rather by the science editors, who consult with selected external editors and reviewers.

Citation for this article: *J Clin Invest.* doi:10.1172/JCI73441.

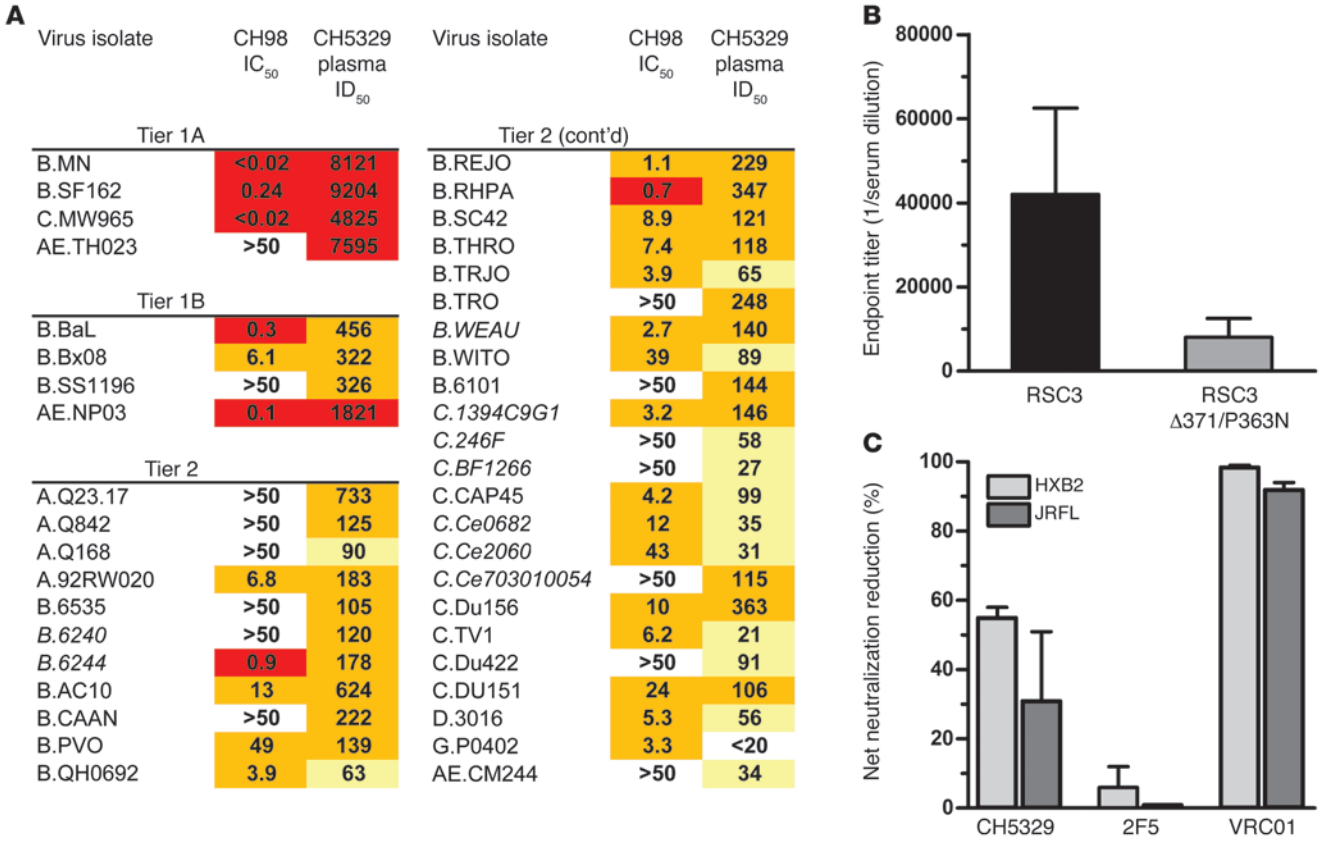

Figure 1

Identification of neutralizing CD4bs antibodies in CH5329 serum. (**A**) CH5329 plasma and mAb CH98 neutralization profiles, measured as ID_{50} and IC_{50},respectively, in TZM-bl assay. Transmitted/founder HIV-1 isolates are italicized. For plasma neutralization: red, ID_{50} >1,000; orange, ID_{50} 100 to 1,000; yellow, ID_{50} >20 and <100; white, ID_{50} <20 (absence of neutralization). For CH98 BnAb: red, IC_{50} <1 μg/ml; orange, IC_{50} 1 to 50 μg/ml; white, IC_{50} >50 μg/ml (absence of neutralization). (**B**) Differential binding by CH5329 serum to the RSC3 protein and the CD4bs knockout RSC3Δ371I/P363N, graphed as ELISA endpoint titer (final reciprocal serum dilution with background-corrected OD ≥0.1). (**C**) CD4bs-directed neutralizing activity in CH5329 serum, shown as percent reduction in ID_{80} in the presence of RSC3 compared with the knockout RSC3Δ371I/P363N against HIV-1 JRFL and HxB2 strains. Values for the BnAbs VRC01 and 2F5 are included as positive and negative control, respectively. In **B** and **C**, error bars represent SEM from 2 independent experiments.

oping BnAbs in the context of their autoreactive humoral response (24, 26–28). The observations that HIV-1 infection is reported with a disproportionately low frequency among subjects with SLE support this hypothesis (29–34).

To date, there have been no reports of studies of the HIV-1 antibody repertoire of SLE subjects from whom BnAbs have been isolated. Here, we describe CH98, an HIV-1 CD4bs BnAb isolated from an HIV-1–infected individual with SLE (subject CH5329; see Methods). CH98 displayed a number of unusual antibody traits shared by autoimmune disease autoantibodies.

Results

CH5329 plasma neutralization and isolation of CH98. In a multiclade, multitier panel of HIV-1 strains, consisting of 4 tier-1A, 4 tier-1B, and 34 tier-2 isolates, including 9 transmitted/founder viruses, plasma from subject CH5329 neutralized 41 of 42 HIV-1 strains (97.6%), with a mean ID_{50} titer of 925 (range, 21–9,204; Figure 1A). The only HIV-1 strain that was not neutralized, G.P0402, was a clade G. CH5329 plasma was screened in 2 different but complementary assays for CD4bs activity. CH5329 plasma bound to the HIV-1 Env resurfaced core 3 (RSC3) protein with a mean endpoint titer 5-fold higher than that of the RSC3Δ371I/P363N protein (Figure 1B and Supplemental Figure 1; supplemental material available online with this article; doi:10.1172/JCI73441DS1), indicative of the presence of CD4bs mAbs (7). The RSC3 protein preferentially blocked the neutralization ability of CD4bs mAbs such as VRC01, but not mAbs directed against other sites, such as the gp41-binding 2F5 BnAb. However, the ability of RSC3 protein to block neutralizing activity in HIV-infected sera is rare (35) and indicative of the presence of CD4bs neutralizing antibodies (7, 8). Therefore, the 30%–55% reduction we observed in total serum neutralization against 2 different HIV-1 strains, HxB2 and JRFL (Figure 1C), indicated that CD4bs antibodies markedly contribute to plasma neutralization.

mAb CH98 V_HDJ_H and V_LJ_L gene segments were isolated from a clonal memory B cell culture containing 29 ng/ml IgG at the end of stimulation with culture supernatant that bound to RSC3 but not RSC3Δ371I, and were expressed as a full recombinant IgG1 mAb (11, 36, 37). CH98 neutralized 27 of 43 HIV-1 isolates (62.8%), with a median IC_{50} neutralization level of 4.2 μg/ml (range, <0.02–49 μg/ml), accounting for 65.9% of the observed plasma neutralization breadth (Figure 1A). No other antibodies were retrieved that bound to RSC3 or neutralized the A.Q23.17 HIV-1 strain,

which was selected to screen culture supernatants for heterologous neutralizing activity (see Methods). Thus, the frequency of peripheral blood circulating CD4bs neutralizing antibodies in this subject was estimated to be 0.003%.

Characteristics of CH98. CH98 uses the V_H3–30 gene segment, notably not the V_H1–2 or V_H1–46 segments commonly associated with VRC01-like CD4bs BnAbs (8, 9), paired with the $V_\lambda2$–23 light chain gene segment. CH98 is highly mutated, with V_HDJ_H and V_LJ_L mutation frequencies of 25.3% and 15.8%, respectively, and displays a long HCDR3 of 21 aa (Supplemental Table 1). From 454 pyrosequencing, we identified 4 additional V_HDJ_H rearrangements in the CH98 clonal lineage, and all were highly mutated and shared numerous mutations with the CH98 V_HDJ_H (Supplemental Figures 2 and 3).

The CH98 light chain CDR 1 (LCDR1) is 27 nt long and underwent a 15-nt deletion preceded by an activation-induced cytidine deaminase (AID) hotspot (AGT; Supplemental Figure 4). TGT motifs are also present near the start and the end of this deletion (Supplemental Figure 4), raising the hypothesis that slipped-strand synthesis may have occurred at this position. It is also worth noting that the CH98 V_L/J_L gene segment rearrangement had a very long *n*-region insertion of 24 nt in the LCDR3 that were not encoded by either of the V_L2–23 or J_L3 germline sequences (Supplemental Figure 4).

CH98 epitope mapping. CH98 bound to RSC3 protein (IC_{50}, 0.51 μg/ml), but not to RSC3Δ371I/P363N; in contrast to the CD4bs BnAb VRC01, CH98 did not bind to RSC3 G367R mutant or to the gp120 outer domain stabilized protein OD4.0 (Supplemental Table 2). Binding to WT YU2 gp120 Env (IC_{50}, 0.03 μg/ml) was abrogated by the D368R mutation, which disrupts a key contact residue within the CD4bs, but not by the I420R mutation (IC_{50}, 0.11 μg/ml), which disrupts the CCR5 coreceptor binding site (Supplemental Table 2). Also, CH98 potently neutralized the HIV-1 YU2 strain (IC_{50}, 0.9 μg/ml). Therefore, we epitope mapped CH98 on a panel of YU2 gp120 core protein mutants previously used to map other mAbs binding within and outside the CD4bs (38, 39). We compared the binding profile of CD4bs BnAb CH98 with those of other CD4bs BnAbs — CH103 (4), VRC01 (7), CH31–CH34 (8), and b12 (5, 6) — as well as non-neutralizing CD4bs b6 mAb and CD4-Fc to 31 YU2 gp120 core single-point mutants (Figure 2). Single-point mutations outside the CD4bs did not affect CH98 binding. Within the CD4bs, mutations in position 365 and 368 abrogated binding of all CD4bs BnAbs tested, but not mAb b6, and mutations in positions 282, 461, and 473 reduced CH98 binding to 55%, 64%, and 31%, respectively (Figure 2). Overall, CH98 was the BnAb least sensitive to the mutations represented in the panel, which indicates that these positions are less relevant for CH98 binding to its cognate epitope than for the other CD4bs BnAbs. The only antibodies sensitive to all the mutations that also affected CH98 binding were the BnAbs CH103 and VRC01.

Comparison of CH98 with CD4bs mAbs CH103 and VRC01. CH103 and VRC01 bind to the CD4bs with 2 distinct modes of epitope recognition: CH103 uses a loop dominated mode of interaction including all V_HDJ_H and V_LJ_L CDRs (4), whereas VRC01 contacts the CD4bs by mimicking CD4 with a large footprint that is dominated by HCDR2 and encompasses both heavy and light chains (40). To determine whether CH98 falls into one of these categories, we threaded the CH98 heavy and light chains onto the gp120-complexed structure coordinates of CH103 (4) and VRC01 (40).

CH98 threading on the VRC01 gp120-complexed structure resulted in steric clashes between the LCDR3 of CH98 and the D loop of gp120 (Figure 3A). Relaxation of the model to alleviate the

% Binding (normalized to WT)

YU2 gp120 core	CH98	CH103	VRC01	CH31	CH32	CH33	CH34	b12	CD4-Fc	b6
WT	100	100	100	100	100	100	100	100	100	100
K121T	99	114	83	87	91	90	89	92	100	102
N197K	96	146	79	97	89	90	95	89	96	98
V200K	102	164	87	78	92	95	97	94	103	95
H216Y	103	131	89	101	97	108	100	108	127	102
K231T	97	70	77	88	83	138	87	98	84	98
T240K	106	115	91	103	98	117	97	101	118	116
L265R	90	57	80	88	81	156	86	91	72	100
E269G	99	96	83	93	92	138	90	95	114	106
T278K	100	150	288	5	3	21	4	89	159	111
K282V	55	44	60	75	89	71	75	51	23	77
G327R	101	100	92	95	92	95	93	90	100	110
Q337V	99	145	76	93	86	90	86	88	100	103
Q344V	95	144	93	95	90	95	90	94	96	101
S365K	7	10	25	52	29	55	45	28	5	110
D368R	1	11	5	4	2	10	3	2	5	76
D397F	93	147	83	92	89	90	102	91	103	105
R403V	88	98	103	88	93	89	86	76	97	104
L405D	93	123	99	92	87	91	91	80	107	100
R412V	94	115	88	92	95	95	93	87	109	102
R419G	91	88	78	82	88	89	82	13	89	101
G434K	96	121	83	88	83	86	88	76	93	99
Q442V	96	86	101	91	84	90	88	72	84	99
S446K	114	91	94	111	106	114	106	113	124	111
T455E	84	499	64	14	17	16	14	14	17	107
G459E	97	10	24	2	2	1	1	105	5	104
D461I	64	16	57	75	91	76	83	78	77	107
I467K	105	38	46	114	88	105	98	51	26	103
G473R	31	38	12	61	26	90	68	113	7	91
R476V	79	64	67	64	85	45	64	97	18	20
K490S	90	84	78	90	85	85	83	89	94	95

0 25 50 75 100 125 150 175

Figure 2
Effect of point mutation of the YU2 core protein on CD4-Fc and on CH98, CH31–CH34, VRC01 and b12 CD4bs BnAbs, and the non-neutralizing CD4bs b6 mAb. The effect of point mutations on the binding to the YU2 core protein of CH98 and other CD4bs mAbs and CD4-Fc is expressed as percentage normalized to binding to the WT YU2 gp120 core protein and color coded as indicated. Positioning within the CD4bs (green), or adjacent or nearby (black), is indicated at far right.

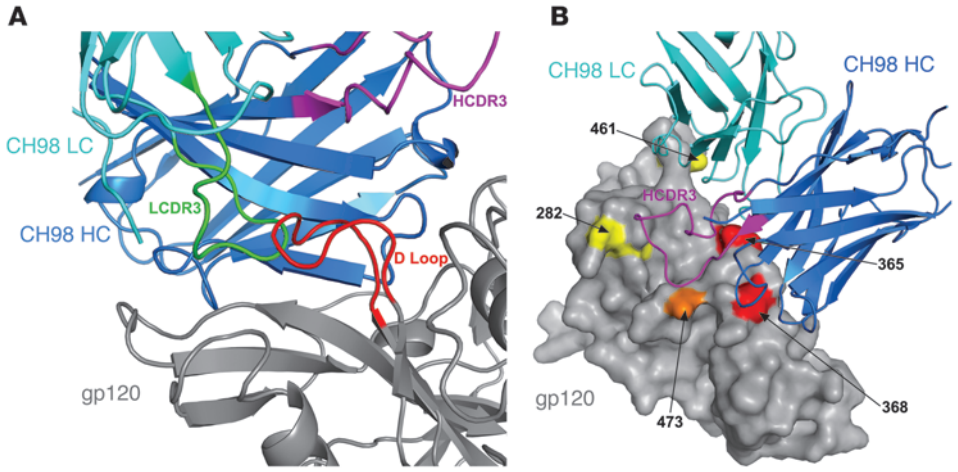

Figure 3
Threading of CH98 onto the gp120 complexed structures of CD4bs VRC01 and CH103 BnAbs. (**A**) CH98 model based on threading onto the gp120 complexed VRC01 crystal structure. The CH98 heavy chain (HC; dark blue) and light chain (LC; light blue) threaded onto the VRC01 structure complexed with gp120 (gray) resulted in an incompatible model, with a clash between the gp120 D loop (red) and the LCDR3 (green). (**B**) CH98 model based on threading onto the gp120 complexed CH103 crystal structure. The CH98 heavy chain (dark blue) and light chain (light blue) threaded onto the CH103 structure complexed with gp120 (gray) resulted in a model in which HCDR3 (magenta) dominates the binding to the CD4bs region and engages in direct contact with gp120 residues in positions 365, 368, 473, and 282, all of which affect CH98 binding. The residue in position 461 makes direct contact with LCDR1. Each residue that affects CH98 binding in the epitope mapping is illustrated using the corresponding color in Figure 2.

clashes resulted in a complex with a binding energy score of –31.96 Rosetta energy units (REU; see Methods), which was higher (i.e., less favorable) than those of both the solved VRC01-gp120 complex and the CH98 complex modeled in the CH103 mode of recognition (–40.84, and –37.86 REU, respectively). Conversely, CH98 threading onto the gp120-complexed CH103 crystal structure resulted in a model compatible with a CH103-like mode of antigen recognition (Figure 3B). Between the 2 mAbs, aa sequence homology was 36% and 56% for the V_HDJ_H and V_LJ_L, respectively (Supplemental Figure 5 and Supplemental Table 3). This model supported the observed binding data (Figure 2) and predicted that all the heavy and light chain CDRs of CH98 make direct contact with the 5 residues affecting CH98 binding to the YU2 gp120 core (Supplemental Table 4).

In particular, D461 was predicted to contact LCDR1 (Supplemental Figure 6A), which is 9 aa long and underwent a 5-aa deletion. Therefore, we asked whether a LCDR1 deletion-reverted CH98 would be compatible with the gp120-complexed CH103 mode of recognition. Adoption of the canonical conformation for a LCDR1 of length 14, as defined by North and colleagues (41), allowed the deletion-reverted LCDR1 to avoid steric clashes at the gp120 interface; however, the binding energy score of the complex was less favorable than that of the mature CH98 complex (–35.09 versus –37.86 REU; Supplemental Figure 6B). Our interpretation is that the 15-nt deletion in the CH98 LCDR1 may have played a favorable role during the process of affinity maturation of CH98.

CH98 BnAb reactivity with human proteins. In a panel of 9 autoantigens associated with presence of autoimmune diseases (Sjogren's syndrome antigens A and B [SSA and SSB, respectively], Smith antigen [Sm], ribonucleoprotein [RNP], centromere B [Cent B], histone, scleroderma 70 [Scl 70] and Jo-1 proteins, and dsDNA), CH98 reacted with dsDNA (Figure 4A). CH98 binding to dsDNA was comparable to that previously observed for the CD4bs BnAb CH103 (Supplemental Figure 7). In the same assay, CH5329 plasma from the same specimen from which CH98 BnAb was isolated was found to be positive for SSA and dsDNA antibodies (mean ± SD, 268 ± 29 and 163 ± 22 response units [RU], respectively; Figure 4B).

In HEp-2 cell IFA staining, CH98 displayed diffuse fine granular cytoplasmic staining, exhibited stronger binding to dividing cells, and bound to intracellular vesicles in a subset of HEp-2 cells (Figure 4, C–E). CH98 reactivity with 9,400 additional human proteins was screened using microarray technology (28). CH98 showed polyreactivity with numerous human antigens, as measured by 1 log stronger binding to more than 90% of the test proteins than the non-polyreactive control antibodies 151K and palivizumab. CH98 also bound with higher affinity, measured as a >2 log increase in binding compared with antibody controls, to STUB1 (also known as CHIP), an E3 ubiquitin-protein ligase (Figure 4, F and G). Binding of CH98 and CH5329 plasma to STUB1 were confirmed in direct-binding ELISA with an endpoint titer of 3.3 μg/ml for CH98 and plasma titer of 270 (Supplemental Figure 8, A and B). We previously demonstrated that members of the CD4bs BnAb CH103 clonal lineage displayed reactivity with dsDNA and with UBE3A, another E3 ubiquitin-protein ligase (4). Such reactivity was also shared by the CD4bs BnAb VRC01 (4). However, these BnAbs did not bind to STUB1, and CH98 did not bind to UBE3A (data not shown).

Taken together, these findings suggested that the immune system dysregulation that allows for production of autoreactive antibodies during SLE may have played a permissive role in the development and maturation of the BnAb CH98. Moreover, the similarities between CH98 and the SLE autoantibodies of long HCDR3 and dsDNA reactivity are suggestive of similar pools of B cells and mechanisms of their origin.

Discussion

Here, we describe an individual who, when studied 14 years after HIV-1 transmission and 6 years after onset of SLE, controlled her viral load off antiretroviral therapy (ART) and developed plasma BnAb activity.

An open question regarding the development of BnAbs in HIV-1–positive subjects is whether acquisition of autoreactivity is a common prerequisite for the development of neutralization breadth. We have previously described the CH103 CD4bs BnAb isolated from an SLE-negative, chronically HIV-1–infected individual and demonstrated that antibodies in the CH103 clonal lineage acquired autoreactivity with a number of autoantigens, including dsDNA,

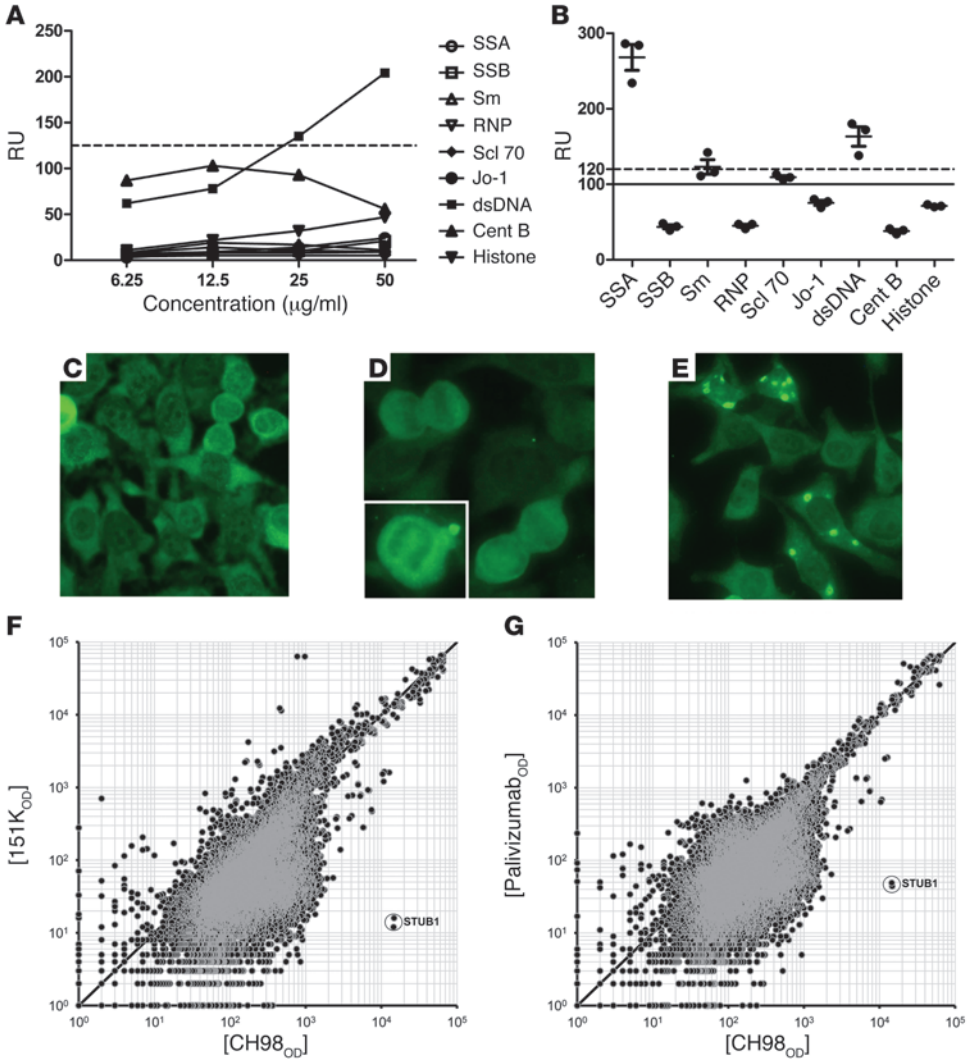

Figure 4
Autoreactivity of CH98. (**A**) CH98 reactivity against common antigens associated with autoimmune diseases, tested with a commercial ANA-II Plus test system. The threshold for positivity was 120 RU (dashed line). (**B**) CH5329 plasma reactivity against common antigens associated with autoimmune diseases, tested with the commercial ANA-II Plus test system. Results from 3 independent experiments are shown. The threshold for negativity was 100 RU (solid line), and that for positivity was 120 RU (dashed line); values of 100–120 RU were considered equivocal specimens. (**C**–**E**) Hep-C IFA staining of BnAb CH98. Antibody concentration was 25 μg/ml, and exposure time was 8 seconds. Original magnification, ×40; inset in **D** is enlarged ×1.5. (**F** and **G**) Reactivity of CH98 on a panel of 9,400 human proteins tested using a ProtoArray 5 microchip, compared with nonautoreactive mAb 151K (**F**) or palivizumab (**G**). Values for STUB1 are encircled.

concurrently with acquisition of HIV-1 neutralization breadth (4). We have also described an individual in whom the onset of gp41 MPER 2F5-like BnAb plasma activity was temporally associated with the development of plasma dsDNA and Jo-1 autoantigen reactivity, without appearance of any clinical manifestation of autoimmune disease (42). Thus, in some individuals, acquisition of BnAb activity is clearly associated with the acquisition of autoreactivity.

Antibodies to dsDNA are a hallmark of SLE and are present in approximately 70% of subjects with SLE, but only 0.5% of SLE-negative individuals (32). Conversely, dsDNA antibodies are not a typical finding during HIV-1 infection, but have been commonly reported in the plasma of the few SLE subjects with HIV-1 infection (30, 33). The presence of plasma dsDNA antibodies has been documented in subjects diagnosed with SLE both after and before HIV-1 diagnosis (91.7% and 64.3%, respectively) (30). The incidence of plasma BnAbs in these reported cases, however, is unknown.

We report herein a monoclonal HIV-1 BnAb, CH98, isolated from a chronically HIV-1–infected individual who subsequently developed SLE. CH98 neutralized HIV-1 through binding to the CD4bs on HIV-1 gp120 and reacted with dsDNA at levels comparable to those previously observed for the CD4bs BnAb CH103. CH98 accounted for only a portion of the plasma neutralization breadth (65.9%). This observation, in conjunction with the finding that RSC3 plasma absorption only partially abrogated plasma neutralization (30%–55%), implies that other neutralizing antibody specificities contributed to the overall plasma neutralization breadth in this individual. These data are in line with previous observations indicating that plasma neutralization breadth can be mediated by a polyclonal response comprising antibodies with distinct specificities and variable degrees of breadth (43–45). Using a combination of epitope mapping and threading of the CH98 heavy and light chains onto the gp120-complexed structure coordinates of CD4bs BnAbs, we determined that CH98 likely uses a CH103-like Env loop mode of epitope recognition that involves all the heavy and light chain CDRs. Conversely, CH98 threading onto the gp120-complexed structure of VRC01 resulted in steric clashes between the LCDR3 of CH98 and the D loop of gp120. This result was not unexpected: VRC01 and all VRC01-like antibodies had unusually short LCDR3s (5 residues), and it has been suggested that the VRC01-like orientation of gp120 binding does not leave enough space between the antibody and the gp120 D loop to accommodate longer LCDR3s (46). Indeed, CH98 has a 12-residue-long LCDR3, and therefore our model is compatible with this hypothesis.

CH98 was also characterized by a short LCDR1 (9 aa) that underwent a 5-aa deletion during the process of affinity maturation. This 15-nt deletion in CH98 LCDR1 was preceded by an AID hotspot. AID hotspots regulate secondary antibody diversification and are directly involved in the process of somatic hypermutation (47, 48). Since we predicted a less favorable binding energy score of the deletion-reverted CH98 complex compared with the mature CH98 complex, our interpretation is that, similar to our prior observation for CH103 (4), a single macromutation may have improved binding to the cognate epitope. In addition, LCDR1s shorter than 11 aa are rare (46), but commonly found among CD4bs BnAbs (4, 46), and both CH103 and VRC01 also have deletions in their LCDR1s (4, 40). We interpret the disproportionate frequency of short LCDR1s among CD4bs BnAbs as being indicative of a common selection process of CD4bs BnAbs that favors antibodies with shortened LCDR1s.

This is the first chronically infected SLE individual with concomitant HIV-1 infection that we have been able to study, and it was striking that this individual also had robust plasma BnAb activity, given that the incidence of chronically HIV-1–infected subjects with this level of plasma neutralization breadth is only approximately 20% (49–52).

In a literature review from 1981 to 2012 by Carugati and colleagues, of 53 HIV-1/SLE patients, 54.7% were diagnosed with HIV-1 before SLE (33). The diagnosis of HIV-1 in our subject preceded that of SLE, and we cannot conclude that the CH98 maturation was initiated as part of the SLE-induced autoreactive response, nor can we exclude the possibility that silent SLE was present before the time of HIV-1 diagnosis.

When generated, BnAbs appear late (2–4 years) after HIV-1 transmission, and serum neutralization breadth correlates with viral load levels (49). This has been interpreted as an indication that persistent antigen stimulation is required to develop neutralization breadth (53–55). In stark contrast, our study subject developed BnAbs while controlling viremia, which suggests that acquisition of HIV-1 neutralization breadth may not always require chronic stimulation with high levels of HIV-1 viremia. A possible explanation is that the maturation of CH98 was not hindered in this subject by immune tolerance control mechanisms, thus facilitating the acquisition of mutations required to achieve neutralization breadth, possibly driven by exposure to both HIV-1 and autoantigens (21, 24, 27). The low viral load and normal CD4 count of this subject while off ART could not be explained by HIV-1–controlling HLA types (56) or by HIV-1 infection with a *nef*-defective strain (57, 58); studies are in progress to determine whether the presence of SLE contributed to virus control.

Kobie and colleagues recently identified an autoreactive plasma antibody population (9G4 anti-idiotype antibodies) that is commonly found in SLE subjects and is responsible for serum HIV-1 neutralization breadth in ART-naive, SLE-negative, chronically HIV-1–infected subjects; the authors proposed that this kind of antibody may derive from the same pool of B cells of SLE-induced antibodies (34). The BnAb CH98 differs from 9G4-positive antibodies in that it uses a V_H3–30 gene segment, not V_H4–34, which defines 9G4 antibodies. Therefore, our findings demonstrated that autoreactive antibody populations beyond 9G4-positive antibodies have the potential to broadly neutralize HIV-1 strains in SLE subjects.

In conclusion, we demonstrated that a virus-controller SLE patient with chronic HIV-1 infection developed the highly mutated CD4bs BnAb CH98, and this antibody displayed characteristics typical of SLE-induced autoantibodies. Our findings support the hypothesis that lax mechanisms of tolerance control associated with SLE may have favored the maturation of this BnAb by favoring its evasion from deletion during the process of somatic maturation and the acquisition of reactivity with self-antigens. Moreover, our data support the concept that BnAbs develop from a similar pool of B cells as do autoimmune B cells in SLE.

Methods

Patient information. Subject CH5329 is a female patient, aged 33 years at the initiation of the study. At 19 years of age, the patient was diagnosed with HIV-1; at 27 years of age (8 years after HIV-1 diagnosis), the subject was diagnosed with SLE. The patient sought health care at the Duke University Medical Center Clinics in 2009 (age 31 years). At admission, her general health conditions were overall good with no fever, chills, night sweats, nausea, vomiting, or diarrhea. CD4 count was 460 cells/mm^3. She had not received any ART. SLE diagnosis was confirmed at admission based on American College of Rheumatology criteria for SLE (59): malar rash, discoid rash, photosensitivity, arthritis, and presence of plasma speckled anti-nuclear antibody titer of 160. The subject also reported a history of seizures that preceded the diagnosis of both SLE and HIV-1 infection, as well as a history of asthma, which was controlled by daily triamcinolone and albuterol. In 2009, her plasma was negative for SSA, SSB, RNP, Sm, and dsDNA antibody. Serum complement levels were normal. Her SLE was treated with plaquenil from 2005 to January 2008 and 7.5 mg methotrexate once weekly from 2006 to December 2012, when plaquenil was restarted and continued up to date.

The patient was enrolled in 2011 in the CHAVI008A study of chronic HIV-1–infected individuals. Plasma, PBMCs, and leukapheresis samples were collected and studied. At enrollment, the subject had received no ART, and her CD4 count and viral load were 568 cells/mm^3 and 4,150 HIV RNA copies/ml, respectively. Her MHC class I phenotype was HLA-B7 and HLA-B40. Analysis of 64 HIV-1 3′-half genome sequences generated by the single genome amplification method showed the intact *nef* gene in all sequences (Supplemental Figure 9). In 2011, her plasma was positive for dsDNA antibodies; negative for SSA, SSB, Sm, RNP, Scl 70, Jo-1, Cent B, and histone antibodies; and showed an ANA-positive pattern in HEp-2 cell intracellular fluorescence staining with an endpoint titer of 320.

Cell cultures. IgG$^+$ memory cells were isolated from PBMCs as previously described (11). Briefly, IgG$^+$ memory B cells were isolated from frozen PBMCs by 2 rounds of separation using magnetic beads (11). First, PBMCs were incubated for 30 minutes at 4°C with PE-conjugated anti-CD2 (catalog no. 555327), anti-CD14 (catalog no. 555398), anti-CD16 (catalog no. 555407), anti-CD235a (catalog no. 555570), and anti-IgD (catalog no. 555779) antibodies (all from BD Biosciences — Pharmingen), followed by a 15-minute incubation with anti-PE microbeads (Miltenyi Biotec) at 4°C. After washing, cells were passed through magnetic columns using the Deplete_S program of the AutoMACs separator (Miltenyi Biotec). The negative fraction was then incubated for 15 minutes with anti-IgG microbeads (catalog no. 130-047-501; Miltenyi Biotec). After washing, IgG$^+$ memory B cells were selected using the Possel_S program of the AutoMACs separator (11). All steps of the separation procedure were performed using cold PBS with 0.1% BSA buffer (PBSB). IgG$^+$ memory B cells were stimulated for 14 days in vitro to induce proliferation and differentiation into antibody-secreting cells for functional studies on the culture supernatants, using a previously described stimulation protocol (11). Briefly, cells were resuspended in complete medium containing 2.5 μg/ml CpG ODN2006 (tlrl-2006; InvivoGen), 5 μM CHK2 kinase inhibitor (Calbiochem/EMD Chemicals), and EBV (200 μl supernatant of B95-8 cells/10^4 memory B cells) and incubated in bulk overnight at 37°C in 5% CO_2 (11). After overnight incubation, 28,800 viable IgG$^+$ memory B cells were manually trans-

ferred at an average density of 3 cells/well in 96-well round-bottomed tissue culture plates containing ODN2006, CHK2 kinase inhibitor, and 5,000 irradiated (7,500 cGy) CD40 ligand–expressing L cells per well. The cell density of 3 cells per well was chosen to achieve the expansion of a single cell in the majority of wells, according to Poisson distribution and previous experimental observations using this method. Medium was refreshed after 7 days, and supernatants were harvested at day 14 (11). Cell culture supernatants were screened for IgG levels, differential binding to RSC3 and RSC3Δ371I, and neutralization of the clade A.Q23.17 HIV-1 strain. This screening strategy was selected to isolate BnAbs based on the observed plasma differential binding to RSC3 and RSC3Δ371I and the high plasma ID_{50} A.Q23.17 HIV-1 strain neutralization. The RSC3 gp120 core antigen is a protein designed to retain the antigenic structure of the neutralizing surface of the CD4bs while eliminating other antigenic regions of the HIV-1 envelope glycoprotein, and the deletion of a single aa in position 371 (RSC3Δ371I; originally described as ΔRSC3) abrogates or heavily reduces the binding of CD4bs BnAbs (7). Since CD4bs BnAbs such as VRC01, VRC01-like, and CH103 have been previously isolated from memory B cells that bound to RSC3 using antigen-specific cell sorting (4, 7, 44, 60), we decided to use this protein to screen cultured memory B cells cultured to retrieve CD4bs BnAbs using our culture system.

Isolation of V(D)J Ig regions and expression of recombinant antibody. RNA from positive cultures was extracted using standard procedures (RNeasy mini-kit; Qiagen), and the genes encoding Ig V_HDJ_H and V_LJ_L rearrangements were amplified by RT and nested PCR without cloning, using a previously reported method (11, 36). Briefly, reverse transcription was performed at 55°C for 1 hour after the addition of 50 U/reaction of Superscript III RT (Life Technologies) and 0.5 μM human IgG, IgM, IgD, IgA1, IgA2, Igκ, and Igλ constant-region primers. Separate reactions were used to amplify individual families of V_H, $V_κ$, and $V_λ$ genes from the cDNA template; this was performed using 2 rounds of PCR: first round, 5 μl RT reaction product, 5 U HotStar Taq Plus (Qiagen), 0.2 mM deoxynucleoside triphosphates (dNTPs), 0.5 μM nested constant-region primers (IgH consisting of IgM, IgD, IgG, IgA1 and IgA2; Igκ or Igλ), and matched variable-region primers; second round, 2.5 μl first-round reaction product, 5 U HotStar Taq Plus, 0.2 mM dNTPs, 0.5 μM nested constant-region and nested variable-region primers. First-round PCR was cycled as follows: 95°C for 5 minutes; 35 cycles at 95°C for 30 seconds, 55°C (V_H and $V_κ$) or 50°C ($V_λ$) for 60 seconds, and 72°C for 90 seconds; and 1 cycle at 72°C for 7 minutes. Second-round PCR was similar, except that the extension step was performed at 58°C (V_H), 60°C ($V_κ$), or 64°C ($V_λ$). Samples of V_H, $V_κ$, and $V_λ$ chain PCR products were analyzed on 2% agarose gels (Qiagen). Products were sequenced in the forward and reverse directions using a BigDye sequencing kit on an ABI 3700 instrument (Applied Biosystems). Sequence base calling was performed by using Phred. V, D, and J region genes and mutations were analyzed using the SoDA information system (61). All primers used for the second round of PCR included tag sequences at the 5′ end of each primer to permit the assembly of the V_H and V_L genes into functional linear Ig gene expression cassettes by overlapping PCR, as reported elsewhere (36).

Expression of recombinant antibody. Isolated Ig V_HDJ_H/V_LJ_L gene pairs were assembled by PCR into linear full-length Ig heavy- and light-chain gene expression cassettes as previously described (36). The human embryonic kidney cell line 293T (ATCC) was grown to near confluence in 6-well tissue culture plates (BD) and transfected with 2 μg/well purified PCR-produced IgH and IgL linear Ig gene expression cassettes using Effectene (Qiagen). Supernatants were harvested from the transfected 293T cells after 3 days of incubation at 37°C in 5% CO_2.

Neutralization assays. Neutralizing antibody assays with TZM-bl cells were performed as previously described (62). Purified recombinant antibodies were tested starting at a 50-μg/ml final concentration and titrated using serial 3-fold dilutions. Plasma antibody was tested starting at a 1:20 dilution. Pseudotyped lentiviruses were added to the antibody dilutions at a predetermined titer to produce measurable infection and incubated for 1 hour. TZM-bl cells were added and incubated for 48 hours before lysis, after which the supernatant was measured for firefly luciferase (Britelite Plus; Perkin-Elmer) activity using a luminometer. Data were calculated as the reduction in luminescence compared with control wells and reported as IC_{50} (in μg/ml) for purified recombinant antibodies or ID_{50} titer (as 1/dilution) for plasma (62). Plasma neutralization resistance was defined as an ID_{50} titer <20. For further information on the viruses used for neutralization screening, see Supplemental Table 5.

Direct binding ELISAs. Direct binding assays were performed in 384-well plates as previously described (11). Briefly, plates were coated overnight at 4°C with 15 μl purified proteins at optimized concentrations and blocked with assay diluent (PBS containing 4% [w/v] whey protein, 15% normal goat serum, 0.5% Tween 20, and 0.05% sodium azide) for 2 hours at room temperature. Primary culture supernatants were screened at a 1:3 dilution in assay diluent, whereas purified recombinant antibodies were tested using 3-fold serial dilutions starting at 100 μg/ml. 10 μl of primary antibodies were added to each well and incubated for 2 hours at room temperature. Plates were developed using 15 μl/well horseradish peroxidase–conjugated goat anti-human IgG Fc (catalog no. 109-035-098; Jackson ImmunoResearch Laboratories) at a 1:9,000 dilution in 5% goat serum and PBS for 1 hour, followed by 30 μl/well of SureBlue Reserve TMB One Component microwell peroxidase substrate (catalog no. 53-00-03; KPL). Development was stopped with 15 μl/well of 0.1 M HCl, and plates were read at OD_{450} with a VersaMax microplate reader (Molecular Devices).

HEp-2 cell staining. Indirect immunofluorescence binding of mAbs or plasma to HEp-2 cells (Zeuss Scientific) was performed as previously described (24). Briefly, 20 μl of antibody at 50 μg/ml or plasma in serial dilutions was aliquoted onto a predetermined spot on the surface of a slide (ANA HEp-2 kit). After incubation for 25 minutes at room temperature and washes, 20 μl of secondary antibody (goat anti-human Ig FITC at 20 μg/ml; Southern Biotech) was added to each spot and incubated in a humid chamber for 25 minutes in the dark. After washing and drying, a drop of 33% glycerol was added to each spot, and the slide was covered with a 24- by 60-mm coverslip. Images were taken on an Olympus AX70 instrument with a SpotFlex FX1520 CCD and with a UPlanFL 40× 0.75-NA objective at 25°C in the FITC channel using SPOT software. All images were acquired for 8 or 10 seconds. Image layout and scaling were performed with Adobe Photoshop without image manipulation.

Antibody reactivity against human host cellular antigens. Binding of CH98 to human host cellular antigens was performed using a ProtoArray 5 microchip (Life Technologies) according to the manufacturer's instructions. In brief, ProtoArray 5 microchips were blocked and exposed to 2 μg/ml CH98 or a human myeloma protein (151 K; Southern Biotech), or palivizumab for 90 minutes at 4°C. Protein-antibody interactions were detected by 1 μg/ml Alexa Fluor 647–conjugated anti-human IgG. The arrays were scanned at 635 nm with 10-μm resolution, using 100% power and 600 gain (GenePix 4000B scanner; Molecular Devices). Fluorescence intensities were quantified using GenePix Pro 5.0 (Molecular Devices). Lot-specific protein spot definitions were provided by the microchip manufacturer and aligned to the image.

Epitope mapping. A panel of 32 HIV-1 YU2 gp120 core mutants displayed on *S. cerevisiae* (38) was probed for binding to CD4bs mAbs and CD4-Fc (Sino Biological). For each core mutant, 600,000 induced yeast cells were incubated with anti-HA Ab clone 16B12 (Covance) to detect expression and CD4bs mAbs or CD4-Fc in 50 μl PBSB in black 96-well plates (Greiner Bio One) for 1 hour at room temperature while shaking. Yeast cells were washed twice with 200 μl cold PBSB and subsequently incubated with goat anti-mouse and anti-human detection antibodies conjugated to

Alexa Fluor 488 or Alexa Fluor 647 (Life Technologies) in 50 μl PBSB for 20 minutes shaking at room temperature and covered from light. Yeast cells were washed once as above, suspended in 200 μl PBSB, and analyzed for fluorescence using a MACSQuant (Miltenyi Biotec) flow cytometer. For each mutant, 10,000 events were gated on HA signal, and median fluorescence intensities (MFIs) were determined and normalized for expression. This method has been previously used to test approximately 2 dozen mAbs (binding within and outside the CD4bs), and the observed results were consistent both with crystal structures whenever they were available and with epitope maps generated by other means, whether or not the cocrystals/other maps were generated with YU2 (38, 39). Additionally, fine specificity differences in the residues identified as involved in binding for multiple antibodies have been found to correlate with either broad or narrow neutralization activity (S.K. Grimm and M.E. Ackerman, unpublished observations), further supporting the validity of the method.

CH98 homology modeling. Homology models of CH98 in complex with gp120 were built using Rosetta protein modeling software (63). The sequence of the heavy and light chains of CH98 were threaded independently onto the template's (CH103, ref. 4; VRC01, ref. 40) heavy and light chain structures (PDB codes 4JAN and 3NGB, respectively). The best-scoring heavy and light chain models from the independent threading runs were then superposed onto the paired heavy and light chain template, and this model was allowed to relax using the Rosetta FastRelax protocol. After relaxation, the model was minimized with AMBER (64). This homology model of the unliganded antibody was then superposed into the solved antibody-gp120 complex structure. The Rosetta loop refinement protocol (65) was used to allow for loop flexibility in the V5 loop of gp120 (a superposition of solved gp120 structures from the PDB indicated the V5 loop to be the most flexible loop in the CD4 binding site) and the HCDR3 loop (the most flexible of the 6 CDR loops; ref. 66). The top-scoring complex model after loop refinement then underwent a last round of relaxation with Rosetta to further refine the complex. A model of the LCDR1 deletion-reverted CH98 complex was built using the above homology modeling procedure using the CH98 mature light chain sequence with the 5-aa GSYNL insertion in LCDR1. One additional step was added to the procedure that placed the LCDR1 in its canonical conformation based on length and sequence using the CDR structural definitions of North and colleagues (41). Predicted binding energy scores for all modeled complexes were computed in Rosetta by subtracting the energy score of the antibody and gp120 alone from the energy score of the antibody-gp120 complex and expressed as REU.

Preparation of libraries for 454 DNA pyrosequencing. V, D, and J segments of the Ig heavy chain were amplified and sequenced using the 454 pyrosequencing platform as previously described (8). Briefly, a cDNA library was constructed by isolation of mRNA from 22 × 10^6 PBMCs using the Oligotex kit (Qiagen) and concentrated to 26 μl in elution buffer. Reverse transcription was performed in 2 35-μl reactions (13 μl mRNA, 3 μl oligo(dT)12–18 at 0.5 μg/μl [Invitrogen], 7 μl 5× first-strand buffer [Invitrogen], 3 μl RNase Out [Invitrogen], 3 μl 0.1M DTT, 3 μl dNTP mix, each at 10 mM, and 3 μl SuperScript II [Invitrogen]) and incubated at 42°C for 2 hours. The cDNA was combined, purified, and eluted in 20 μl elution buffer (NucleoSpin Extract II kit; Clontech). Heavy and light chain variable region rearrangements were amplified by PCR from 5 μl cDNA as template (the rough equivalent of transcripts from 5.5 × 10^6 PBMCs) using the Phusion High Fidelity enzyme (New England Biolabs) according to the manufacturer's instructions. The 50 μl reaction mix was composed of water, 10 μl 5× buffer, 1 μl dNTP mix, each at 10 mM, 1 μl of each primer at 25 μM, and 1 μl enzyme. Gene-specific forward primers for VH3 gene amplification were VH3 Leader A, C, D, E, and F, and the reverse primers were 3′Cγ-CH1 and 3′Cμ-CH1 (8, 67). The forward primer for VL2 amplification was 5′L-VL1/2-5′-GCACAGGGTCCTGGGCCCAGTCTG-3′, and the reverse primer was 3′CL-5′-CACCAGTGTGGCCTTGTTGGCTTG-3′. The PCR cycling program was run according to Phusion enzyme instructions, using 55°C as the annealing temperature for the heavy chain reaction and 66°C for the lambda. The PCR products at the expected size (450–500 bp) were gel purified (Qiagen), followed by phenol/chloroform extraction. 454 pyrosequencing of the PCR products was performed on a GS FLX sequencing instrument (Roche-454; Life Sciences) using the manufacturer's suggested methods and reagents.

Statistics. Values were expressed as mean ± SEM of 2 independent experiments where indicated. Statistical analysis was performed using GraphPad Prism 5 (GraphPad Software).

Study approval. This study was approved by the Duke IRB and the NIH NIAID DAIDS PSRC committee. Informed consent was received from the participant prior to inclusion in the study according to U.S. federal, local, and Duke University Medical Center regulations.

Acknowledgments

We thank Krissey Lloyd, Christina Scholarchuk, Julie Blinn, Andrew Foulger, Fangping Cai, Miroslawa Bilska, Morgan Gilman, and Rekha Bhaskarabhatla for excellent technical support; and Kelly A. Soderberg, Megan McCormick, Jennifer Kirchherr, Celia C. LaBranche, and Janet Mueller for project and/or regulatory management and coordination. We thank the NISC Comparative Sequencing Program of the NIH Intramural Sequencing Center, National Human Genome Research Institute, for 454 pyrosequencing. This study was supported by grants from NIH, NIAID, Center for HIV/AIDS Vaccine Immunology (AI067854), and Center for HIV/AIDS Vaccine Immunology–Immunogen Discovery (AI100645).

Received for publication September 27, 2013, and accepted in revised form January 9, 2014.

Address correspondence to: Mattia Bonsignori, Duke Human Vaccine Institute, Duke University Medical Center, 2 Genome Court, MSRB II, Room 4013, Duke Box 103020, Durham, North Carolina 27710, USA. Phone: 919.681.9739; Fax: 919.684.5230; E-mail: mattia.bonsignori@duke.edu.

1. Bonsignori M, et al. HIV-1 antibodies from infection and vaccination: insights for guiding vaccine design. *Trends Microbiol.* 2012;20(11):532–539.
2. Buchacher A, et al. Generation of human monoclonal antibodies against HIV-1 proteins; electrofusion and Epstein-Barr virus transformation for peripheral blood lymphocyte immortalization. *AIDS Res Hum Retroviruses.* 1994;10(4):359–369.
3. Calarese DA, et al. Dissection of the carbohydrate specificity of the broadly neutralizing anti-HIV-1 antibody 2G12. *Proc Natl Acad Sci U S A.* 2005; 102(38):13372–13377.
4. Liao HX, et al. Co-evolution of a broadly neutralizing HIV-1 antibody and founder virus. *Nature.* 2013; 496(7446):469–476.
5. McInerney TL, McLain L, Armstrong SJ, Dimmock NJ. A human IgG1 (b12) specific for the CD4 binding site of HIV-1 neutralizes by inhibiting the virus fusion entry process, but b12 Fab neutralizes by inhibiting a postfusion event. *Virology.* 1997; 233(2):313–326.
6. Roben P, et al. Recognition properties of a panel of human recombinant Fab fragments to the CD4 binding site of gp120 that show differing abilities to neutralize human immunodeficiency virus type 1. *J Virol.* 1994;68(8):4821–4828.
7. Wu X, et al. Rational design of envelope identifies broadly neutralizing human monoclonal antibodies to HIV-1. *Science.* 2010;329(5993):856–861.
8. Wu X, et al. Focused evolution of HIV-1 neutralizing antibodies revealed by structures and deep sequencing. *Science.* 2011;333(6049):1593–1602.
9. Scheid JF, et al. Sequence and structural convergence of broad and potent HIV antibodies that mimic CD4 binding. *Science.* 2011;333(6049):1633–1637.
10. Corti D, et al. Analysis of memory B cell responses and isolation of novel monoclonal antibodies with neutralizing breadth from HIV-1-infected individuals. *PLoS One.* 2010;5(1):e8805.

11. Bonsignori M, et al. Analysis of a clonal lineage of HIV-1 envelope V2/V3 conformational epitope-specific broadly neutralizing antibodies and their inferred unmutated common ancestors. *J Virol*. 2011;85(19):9998–10009.
12. Walker LM, et al. Broad and potent neutralizing antibodies from an African donor reveal a new HIV-1 vaccine target. *Science*. 2009;326(5950):285–289.
13. Walker LM, et al. Broad neutralization coverage of HIV by multiple highly potent antibodies. *Nature*. 2011;477(7365):466–470.
14. Klein F, et al. Broad neutralization by a combination of antibodies recognizing the CD4 binding site and a new conformational epitope on the HIV-1 envelope protein. *J Exp Med*. 2012;209(8):1469–1479.
15. Muster T, et al. A conserved neutralizing epitope on gp41 of human immunodeficiency virus type 1. *J Virol*. 1993;67(11):6642–6647.
16. Conley AJ, et al. Neutralization of divergent human immunodeficiency virus type 1 variants and primary isolates by IAM-41-2F5, an anti-gp41 human monoclonal antibody. *Proc Natl Acad Sci U S A*. 1994; 91(8):3348–3352.
17. Stiegler G, et al. A potent cross-clade neutralizing human monoclonal antibody against a novel epitope on gp41 of human immunodeficiency virus type 1. *AIDS Res Hum Retroviruses*. 2001; 17(18):1757–1765.
18. Huang J, et al. Broad and potent neutralization of HIV-1 by a gp41-specific human antibody. *Nature*. 2012;491(7424):406–412.
19. Zwick MB, et al. Broadly neutralizing antibodies targeted to the membrane-proximal external region of human immunodeficiency virus type 1 glycoprotein gp41. *J Virol*. 2001; 75(22):10892–10905.
20. Haynes BF, Kelsoe G, Harrison SC, Kepler TB. B-cell-lineage immunogen design in vaccine development with HIV-1 as a case study. *Nat Biotechnol*. 2012;30(5):423–433.
21. Verkoczy L, Kelsoe G, Moody MA, Haynes BF. Role of immune mechanisms in induction of HIV-1 broadly neutralizing antibodies. *Curr Opin Immunol*. 2011; 23(3):383–390.
22. Mouquet H, Nussenzweig MC. Polyreactive antibodies in adaptive immune responses to viruses. *Cell Mol Life Sci*. 2012;69(9):1435–1445.
23. Mouquet H, et al. Polyreactivity increases the apparent affinity of anti-HIV antibodies by heteroligation. *Nature*. 2010;467(7315):591–595.
24. Haynes BF, et al. Cardiolipin polyspecific autoreactivity in two broadly neutralizing HIV-1 antibodies. *Science*. 2005;308(5730):1906–1908.
25. Verkoczy L, et al. Rescue of HIV-1 broad neutralizing antibody-expressing B cells in 2F5 VH x VL knockin mice reveals multiple tolerance controls. *J Immunol*. 2011;187(7):3785–3797.
26. Verkoczy L, et al. Induction of HIV-1 broad neutralizing antibodies in 2F5 knock-in mice: selection against membrane proximal external region-associated autoreactivity limits T-dependent responses. *J Immunol*. 2013;191(5):2538–2550.
27. Haynes BF, Moody MA, Verkoczy L, Kelsoe G, Alam SM. Antibody polyspecificity and neutralization of HIV-1: a hypothesis. *Hum Antibodies*. 2005; 14(3–4):59–67.
28. Yang G, et al. Identification of autoantigens recognized by the 2F5 and 4E10 broadly neutralizing HIV-1 antibodies. *J Exp Med*. 2013;210(2):241–256.
29. Barthel HR, Wallace DJ. False-positive human immunodeficiency virus testing in patients with lupus erythematosus. *Semin Arthritis Rheum*. 1993; 23(1):1–7.
30. Palacios R, Santos J, Valdivielso P, Marquez M. Human immunodeficiency virus infection and systemic lupus erythematosus. An unusual case and a review of the literature. *Lupus*. 2002;11(1):60–63.
31. Mylonakis E, Paliou M, Greenbough TC, Flaningan TP, Letvin NL, Rich JD. Report of a false-positive HIV test result and the potential use of additional tests in establishing HIV serostatus. *Arch Intern Med*. 2000;160(15):2386–2388.
32. Calza L, Manfredi R, Colangeli V, D'Antuono A, Passarini B, Chiodo F. Systemic and discoid lupus erythematosus in HIV-infected patients treated with highly active antiretroviral therapy. *Int J STD AIDS*. 2003;14(5):356–359.
33. Carugati M, et al. Systemic lupus erythematosus and HIV infection: a whimsical relationship. Reports of two cases and review of the literature. *Clin Rheumatol*. 2013;32(9):1399–1405.
34. Kobie JJ, et al. 9G4 autoreactivity is increased in HIV-infected patients and correlates with HIV broadly neutralizing serum activity. *PLoS One*. 2012; 7(4):e35356.
35. Lynch RM, et al. The development of CD4 binding site antibodies during HIV-1 infection. *J Virol*. 2012; 86(14):7588–7595.
36. Liao HX, et al. High-throughput isolation of immunoglobulin genes from single human B cells and expression as monoclonal antibodies. *J Virol Methods*. 2009;158(1–2):171–179.
37. Bonsignori M, et al. Antibody-dependent cellular cytotoxicity-mediating antibodies from an HIV-1 vaccine efficacy trial target multiple epitopes and preferentially use the VH1 gene family. *J Virol*. 2012; 86(21):11521–11532.
38. Mata-Fink J, et al. Rapid conformational epitope mapping of anti-gp120 antibodies with a designed mutant panel displayed on yeast. *J Mol Biol*. 2013; 425(2):444–456.
39. Sundling C, et al. High-resolution definition of vaccine-elicited B cell responses against the HIV primary receptor binding site. *Sci Transl Med*. 2012; 4(142):142ra196.
40. Zhou T, et al. Structural basis for broad and potent neutralization of HIV-1 by antibody VRC01. *Science*. 2010;329(5993):811–817.
41. North B, Lehmann A, Dunbrack RL, Dunbrack RL Jr. A new clustering of antibody CDR loop conformations. *J Mol Biol*. 2011;406(2):228–256.
42. Shen X, et al. In vivo gp41 antibodies targeting the 2F5 monoclonal antibody epitope mediate human immunodeficiency virus type 1 neutralization breadth. *J Virol*. 2009;83(8):3617–3625.
43. Bonsignori M, et al. Two distinct broadly neutralizing antibody specificities of different clonal lineages in a single HIV-1-infected donor: implications for vaccine design. *J Virol*. 2012;86(8):4688–4692.
44. Scheid JF, et al. Broad diversity of neutralizing antibodies isolated from memory B cells in HIV-infected individuals. *Nature*. 2009;458(7238):636–640.
45. Mouquet H, et al. Memory B cell antibodies to HIV-1 gp140 cloned from individuals infected with clade A and B viruses. *PLoS One*. 2011;6(9):e24078.
46. West AP, West AP Jr, Diskin R, Nussenzweig MC, Bjorkman PJ. Structural basis for germ-line gene usage of a potent class of antibodies targeting the CD4-binding site of HIV-1 gp120. *Proc Natl Acad Sci U S A*. 2012;109(30):E2083–E2090.
47. Muramatsu M, Kinoshita K, Fagarasan S, Yamada S, Shinkai Y, Honjo T. Class switch recombination and hypermutation require activation-induced cytidine deaminase (AID), a potential RNA editing enzyme. *Cell*. 2000;102(5):553–563.
48. Oppezzo P, Dighiero G. What do somatic hypermutation and class switch recombination teach us about chronic lymphocytic leukaemia pathogenesis? *Curr Top Microbiol Immunol*. 2005;294:71–89.
49. Gray ES, et al. The neutralization breadth of HIV-1 develops incrementally over four years and is associated with CD4+ T cell decline and high viral load during acute infection. *J Virol*. 2011; 85(10):4828–4840.
50. Simek MD, et al. Human immunodeficiency virus type 1 elite neutralizers: individuals with broad and potent neutralizing activity identified by using a high-throughput neutralization assay together with an analytical selection algorithm. *J Virol*. 2009; 83(14):7337–7348.
51. Gray ES, et al. Antibody specificities associated with neutralization breadth in plasma from human immunodeficiency virus type 1 subtype C-infected blood donors. *J Virol*. 2009;83(17):8925–8937.
52. Tomaras GD, et al. Polyclonal B cell responses to conserved neutralization epitopes in a subset of HIV-1-infected individuals. *J Virol*. 2011; 85(21):11502–11519.
53. Doria-Rose NA, et al. Breadth of human immunodeficiency virus-specific neutralizing activity in sera: clustering analysis and association with clinical variables. *J Virol*. 2010;84(3):1631–1636.
54. Mikell I, Sather DN, Kalams SA, Altfeld M, Alter G, Stamatatos L. Characteristics of the earliest cross-neutralizing antibody response to HIV-1. *PLoS Pathog*. 2011;7(1):e1001251.
55. Piantadosi A, et al. Breadth of neutralizing antibody response to human immunodeficiency virus type 1 is affected by factors early in infection but does not influence disease progression. *J Virol*. 2009; 83(19):10269–10274.
56. Kaslow RA, et al. Influence of combinations of human major histocompatibility complex genes on the course of HIV-1 infection. *Nat Med*. 1996; 2(4):405–411.
57. Kirchhoff F, Greenough TC, Brettler DB, Sullivan JL, Desrosiers RC. Brief report: absence of intact nef sequences in a long-term survivor with nonprogressive HIV-1 infection. *N Engl J Med*. 1995; 332(4):228–232.
58. Learmont JC, et al. Immunologic and virologic status after 14 to 18 years of infection with an attenuated strain of HIV-1. A report from the Sydney Blood Bank Cohort. *N Engl J Med*. 1999; 340(22):1715–1722.
59. Tan EM, et al. The 1982 revised criteria for the classification of systemic lupus erythematosus. *Arthritis Rheum*. 1982;25(11):1271–1277.
60. Scheid JF, et al. A method for identification of HIV gp140 binding memory B cells in human blood. *J Immunol Methods*. 2009;343(2):65–67.
61. Volpe JM, Cowell LG, Kepler TB. SoDA: implementation of a 3D alignment algorithm for inference of antigen receptor recombinations. *Bioinformatics*. 2006;22(4):438–444.
62. Montefiori DC. Evaluating neutralizing antibodies against HIV, SIV, and SHIV in luciferase reporter gene assays. *Curr Protoc Immunol Chapter*. 2005; 12:Unit12.11.
63. Leaver-Fay A, et al. ROSETTA3: an object-oriented software suite for the simulation and design of macromolecules. *Methods Enzymol*. 2011; 487:545–574.
64. Case DA, et al. AMBER 11. San Francisco, California, USA: Unviersity of California Press; 2010.
65. Mandell DJ, Coutsias EA, Kortemme T. Sub-angstrom accuracy in protein loop reconstruction by robotics-inspired conformational sampling. *Nat Methods*. 2009;6(8):551–552.
66. Wong SE, Sellers BD, Jacobson MP. Effects of somatic mutations on CDR loop flexibility during affinity maturation. *Proteins*. 2011;79(3):821–829.
67. Tiller T, Busse CE, Wardemann H. Cloning and expression of murine Ig genes from single B cells. *J Immunol Methods*. 2009;350(1–2):183–193.